Structural characteristics of ^{144}Nd through γ-ray spectroscopy following inelastic neutron scattering

Sally F. Hicks, C. M. Davoren, and W. M. Faulkner
Department of Physics, University of Dallas, Irving, Texas 75062

J. R. Vanhoy
Department of Physics, United States Naval Academy, Annapolis, Maryland 21402
(Received 12 January 1998)

Excited levels in ^{144}Nd below 3.3 MeV have been studied using the $(n,n'\gamma)$ reaction. Electromagnetic transition probabilities, multipole-mixing and branching ratios, and level spins and parities were deduced from measured γ-ray excitation functions, angular distributions, and Doppler shifts. Mixed-symmetry configurations in low-lying excited states were investigated by comparing experimental electromagnetic transition rates with theoretical calculations made using the interacting boson model and with existing calculations from the quasiparticle phonon model, the cluster vibrator model, and the particle-core coupling model. Fragmentation of the 2^+ mixed-symmetry mode is clearly observed through strong $M1$ transitions into the lowest symmetric 2^+ level and through small $E2/M1$ multipole-mixing ratios. Comparisons with similar measurements on ^{142}Ce reveal that these $N=84$ isotones exhibit strong fragmentation of the mixed-symmetry mode, although it appears to be spread into more levels in ^{144}Nd. Evidence is found to support the assignment of the 2779.0-keV level as the 3^- member of the octupole-quadrupole phonon coupled quintuplet in ^{144}Nd and to propose that this excited mode is shared with the 2606.0-keV state. Two- and three-quadrupole phonon excitations, as well as other members of the quadrupole-octupole quintuplet, are also examined. [S0556-2813(98)06105-6]

PACS number(s): 25.40.Fq, 21.10.Re, 23.20.Lv, 27.60.+j

I. INTRODUCTION

The proximity of ^{144}Nd to the $N=82$ closed neutron shell has made this nucleus the subject of numerous investigations into the role of collective and particle configurations in low-lying nuclear excited levels. Mixed-symmetry excitations and quadrupole-octupole coupled states are two types of collective modes which have received considerable attention in this nucleus, as well as in other $N=84$ isotones. Although ^{144}Nd is the most studied of these isotones, there is still a lack of experimental information available for low-lying excited states.

Existing experimental information can be found in the compilation by Tuli [1] for work prior to 1988. More recent experimental investigations include: Coulomb excitation [2,3], in-beam γ-ray and conversion electron studies (Ref. [4] and references cited therein), proton scattering [5,6], electron scattering [7], γ-ray induced Doppler broadening [8], and nuclear resonance fluorescence [9]. In this work, we extend the detailed experimental information available for ^{144}Nd to 3.3 MeV excitation using the $(n,n'\gamma)$ reaction. New information from this investigation includes electromagnetic transition rates for states having lifetimes in the range of a few femtoseconds to about one picosecond, as well as spins, parities, branching and multipole-mixing ratios.

Mixed-symmetry excitations in these isotones have been investigated theoretically [4,10–14] and experimentally [5,7,9,15,16]. To assess this collective mode, it is necessary to have well-determined level properties for excited states between 2 and 3 MeV, since for spherical nuclei the lowest mixed-symmetry excitations are predicted to lie in this energy range [17]. New information enables us to investigate mixed-symmetry strength in low-lying ^{144}Nd excited levels and the fragmentation of this strength, particularly in 2^+ states, by comparing our experimental results with calculations from the interacting boson model (IBM-2), the quasiparticle phonon model (QPM) [7,14], the cluster vibration model (CVM) [4], and the particle-core coupling model (PCM) [13].

The quintuplet of negative-parity states arising from the coupling of quadrupole- and octupole-vibrational modes should have energies near the sum of $E(2_1^+)$ and $E(3_1^-)$ which is also in the 2–3 MeV excitation region in ^{144}Nd. Candidates for this quintuplet of states have been investigated recently [8,9], but questions remain both regarding members of the quintuplet and the possible energy-splitting of these multiphonon excitations. Newly observed decays into the 2_1^+ and 3_1^- states allow us to investigate further these quadrupole-octupole coupled states and the splitting of the two-phonon 3^- strength into more than one excited level. We also investigate two- and three-quadrupole phonon states.

Recent investigations of ^{142}Ce [16], along with this new experimental information for ^{144}Nd, provide a framework for comparing low-lying excitations in these two $N=84$ isotones and for examining the influence of the two additional protons in ^{144}Nd.

In Sec. II we describe the experimental procedures and data reduction techniques used to extract level information. In Sec. III, we present level discussions for those states in which there is debate about the experimental information. Mixed-symmetry excitations are discussed in Sec. IV and multiphonon excitations in Sec. V. Finally, a summary is presented in Sec. VI.

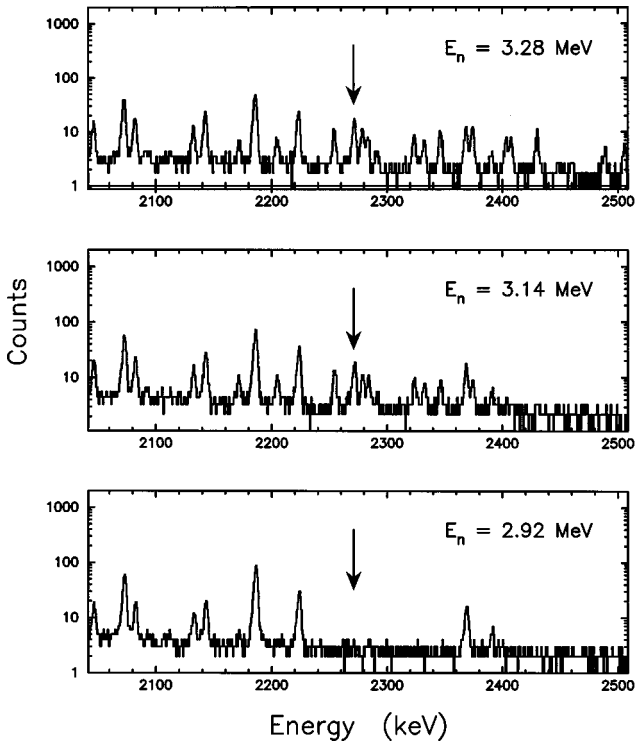

FIG. 1. Gamma-ray excitation function spectra between 2040 and 2510 keV for neutron energies of 2.92, 3.14, and 3.28 MeV. The arrow is drawn at the position of the 2271.9-keV γ ray and shows clearly that this cannot be a ground-state transition. Gamma rays in this portion of the spectrum arise either from ground-state transitions or transitions to the 2_1^+ state.

II. EXPERIMENTAL METHOD AND DATA REDUCTION

Measurements were made using the neutron scattering facility at the University of Kentucky 7 MV Accelerator Laboratory. The ^{3}H$(p,n)^3$He reaction was used as a neutron source. The 41.4 g powdered $^{144}Nd_2O_3$ sample was isotopically enriched to 97.5% and was packed into a thin-walled polyethylene container with a diameter of 3.0 cm and a height of 4.4 cm. Gamma rays were detected with a Compton-suppressed n-type HpGe detector of 52% relative efficiency in a BGO annulus detector. The Ge detector had an energy resolution of 2.1 keV FWHM at 1.33 MeV. The gain stability of the system was monitored at each angle using radioactive ^{56}Co and ^{152}Eu sources. Background lines were identified by scattering from a natural carbon sample. The neutron scattering facilities, time-of-flight background suppression, neutron monitoring, and data reduction techniques have been described elsewhere [18].

Excitation functions measured at 90 degrees for incident neutron energies between 2.2 and 3.3 MeV in 70 keV steps were used to place γ rays in the decay scheme, to determine level energies, and to assist in level spin assignments. Figure 1 shows experimental spectra for γ-ray energies near 2300 keV from the excitation function measurements for neutron energies of 2.92, 3.14, and 3.28 MeV. Experimental excitation function yields were corrected for γ-ray detection efficiency and long counter efficiency as a function of neutron energy in order to obtain relative γ-ray production cross sections. A normalization appropriate for interpreting cross sections was obtained by comparing theoretical cross sections calculated with the statistical model code CINDY [19] and experimental cross sections for 0^+ levels which contained no feeding in these measurements. The CINDY calculations were made using optical model parameters appropriate for this mass and energy region [20]. Experimental γ-ray production cross sections were then compared to theoretical values for levels below about 3.0 MeV to assess level spins and γ-ray branching ratios. Plots of the excitation functions for the 310.8, 1418.1, and 2655.6 γ-ray transitions along with theoretical calculations are shown in Fig. 2. None of the levels represented by these γ rays have adopted spins [1].

Angular distributions of deexcitation γ rays were measured at neutron energies of 2.30 and 3.30 MeV. The angular

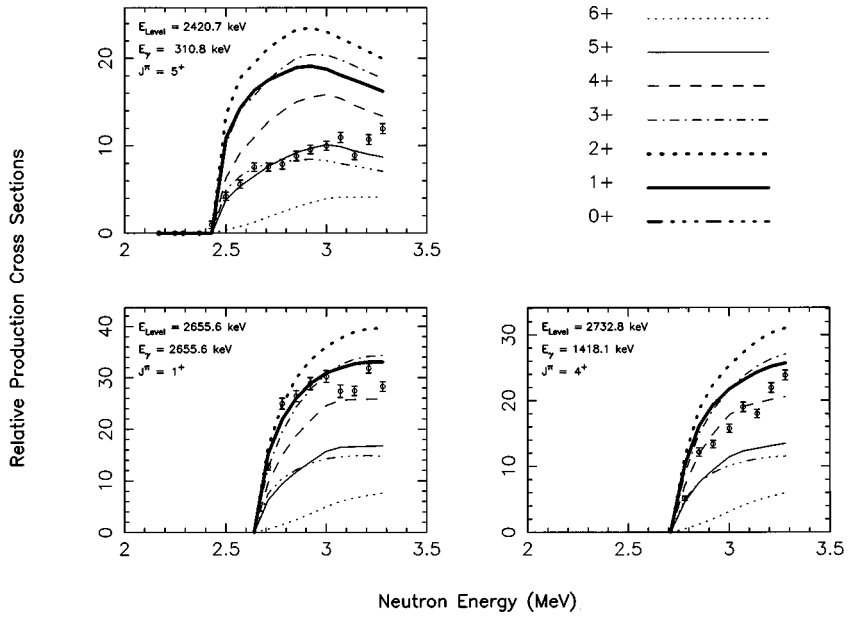

FIG. 2. Gamma-ray excitation functions for the 310.8-, 1418.1- and 2655.6-keV transitions and model γ-ray production cross sections for $J^\pi=(1-6)^+$ for each level. These transitions are from levels whose spins were previously undetermined [1].

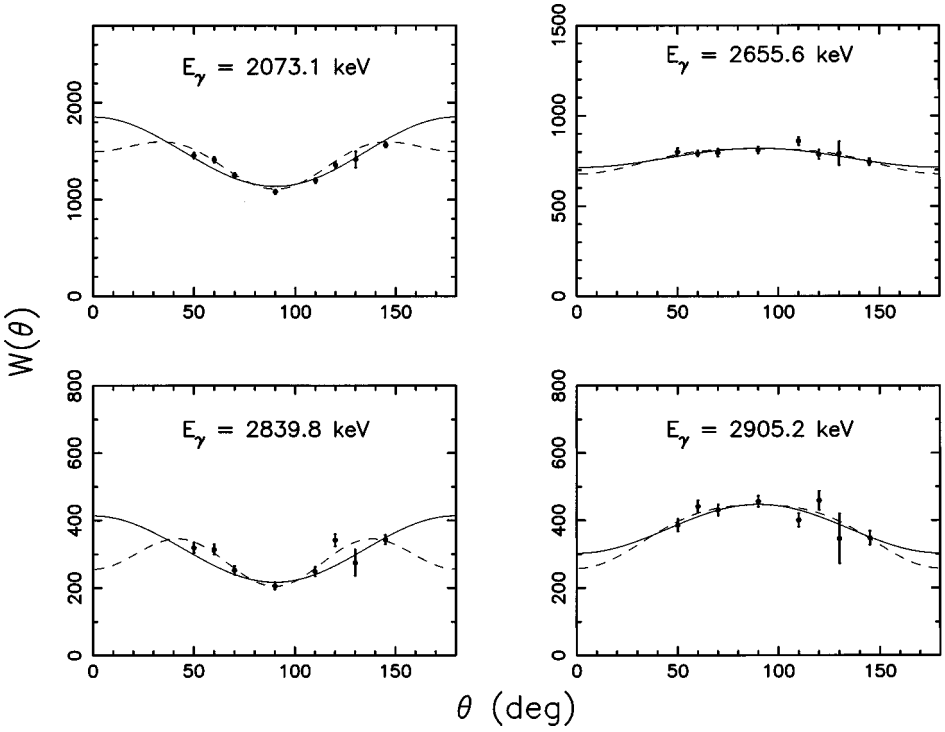

FIG. 3. Angular distributions of four ground-state transitions in ^{144}Nd. The left side of the figure contains angular distributions from levels with $J=2$ and the right side from levels with $J=1$. Curves provided are calculated using a_2 (solid line) and a_2,a_4 (dashed line) coefficients from even-order Legendre polynominal best fits.

distributions were fit to even-order Legendre polynomial expansions and compared to theoretical calculations from CINDY [19] in order to deduce level spins and parities and to extract multipole-mixing ratios. Experimental angular distributions of four ground-state transitions are shown in Fig. 3 along with even-order Legendre-polynomial fits to the data. Figure 4 is an example of the χ^2 vs $\tan^{-1}(\delta)$ plot used to determine the multipole-mixing ratio for the 1003.4 keV transition. Gamma-ray branching ratios were calculated from fits to the angular distributions unless noted otherwise.

Level lifetimes were extracted using the Doppler-shift attenuation method (DSAM) following inelastic neutron scattering. At the recoil velocities present in this experiment, the γ-ray peaks have centroids with the following angular dependence:

$$E_\gamma(\theta)=E_o[1+F(\tau)\beta\cos(\theta)],$$

where E_o is the unshifted γ-ray energy, $F(\tau)$ is the Doppler-shift attenuation factor, $\beta=v_{\text{c.m.}}/c$, θ is the γ-ray emission angle with respect to the incident neutron beam, and $E_\gamma(\theta)$ is the γ-ray energy measured at angle θ. Lifetimes were determined by comparing experimental and theoretical Doppler-shift attenuation factors. Theoretical values of $F(\tau)$ were calculated using the theory of Winterbon [21], since this method has been shown to yield reliable lifetimes with oxide targets [22,23]. Doppler-shift data for the 2655.6-keV ground-state transition are shown in Fig. 5.

Experimental information, including γ-ray intensities, a_2 and a_4 angular distribution coefficients, experimental Doppler-shift attenuation factors, and transition energies, derived from the excitation functions and angular distributions for all observed levels is available from the authors and will be submitted to the Nuclear Data Compilation Center. Electromagnetic transition rates, branching and multipole-mixing ratios, and lifetimes determined from these data are listed in Table I. Newly discovered excited levels are indicated by an ''*h*'' in column four of Table I and new transitions by a ''*g*'' in the same column. Comparisons of our measured transition rates and those from other electromagnetic probes are made in Table II for low-lying 2^+ states and Table III for negative parity states.

III. LEVEL DISCUSSION

Experimental information for all observed levels is provided in the tables; only those states which merit special attention are discussed in detail below.

2072.9-keV 2_3^+ state. Recent investigations of this nucleus by Eckert *et al.* [9,24] listed the spin of this level as $(2,1)^+$. The angular distribution of the ground-state decay of this level is shown in Fig. 3 and clearly has a shape characteristic of $E2$ radiation. The angular distribution of the 1376.3-keV transition also supports the spin-2 assignment of Refs. [6,7].

2109.9-keV 4_2^+ state. Previous (p,p') [6,25] and (e,e') [7] investigations set the spin of this level as 4^+. Cottle *et al.* [5] prefer $J^\pi=2^+$, also from (p,p') investigations. Angular distributions and excitation functions from this $(n,n'\gamma)$ measurement agree with the spin 4 assignment; the observed 310.8-keV transition into this state from the 2420.7 keV 5^+ level further excludes a spin-2 assignment.

(2270-keV state). Two transitions of 2271 and 1573 keV have been assigned to this level [1]. New data show that both the 2271.9-keV and 1573.0-keV γ rays come from higher-lying excitations. Experimental spectra in the region of the

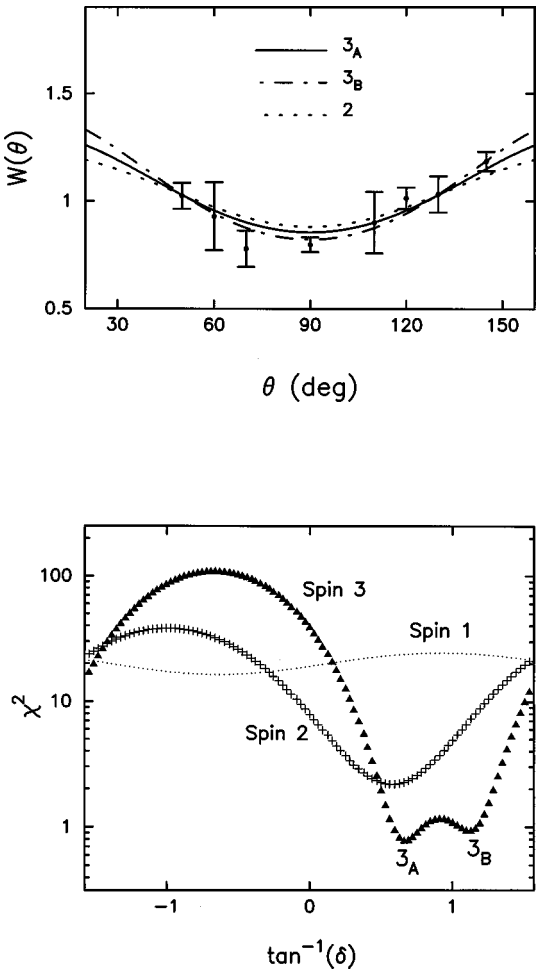

FIG. 4. The top panel is a plot of the angular distribution of the 1003.4-keV transition with curves calculated after determining possible spin-mixing ratio solutions from the lower panel χ^2 vs $\tan^{-1}(\delta)$ plot. In many cases, the correct initial state spin is known only after referring to similar information from other transitions.

2271.9-keV transition are shown in Fig. 1. The arrows in Fig. 1 are drawn at the position of the 2271.9-keV γ ray and show clearly that it cannot be a ground-state transition. No evidence of this level is observed.

2295.5-keV 4^+ state. Five transitions are adopted for this level [1]; all but the 202-keV transition are confirmed in this measurement. Proton scattering experiments by Pignanelli *et al.* [6] indicate the state has $J^\pi=4^+$; however, in other (p,p') measurements [5], as well as in (e,e') investigations [7], this level is not observed. Reference [1] lists $J^\pi=(2,3,4)^+$. Newly measured γ-ray angular distributions for all four observed transitions support J=4.

(*2321-keV state*). One transition of 1007.2 keV has been assigned to this level by Snelling and Hamilton [26]. We observe a weakly excited 1006.0-keV transition with a considerably higher threshold which we place with the 3185.5-keV level. We find no evidence of the 2321-keV state.

2564.3-keV $(3)^+$ state. Three transitions were assigned to this level by Snelling *et al.* [26] from γ-γ coincidence measurements. A transition of 1868.1 keV is observed in our investigation which clearly belongs at 2565 keV. This transition is not adopted [1], although the same assignment was made previously by Al-Janabi *et al.* [25].

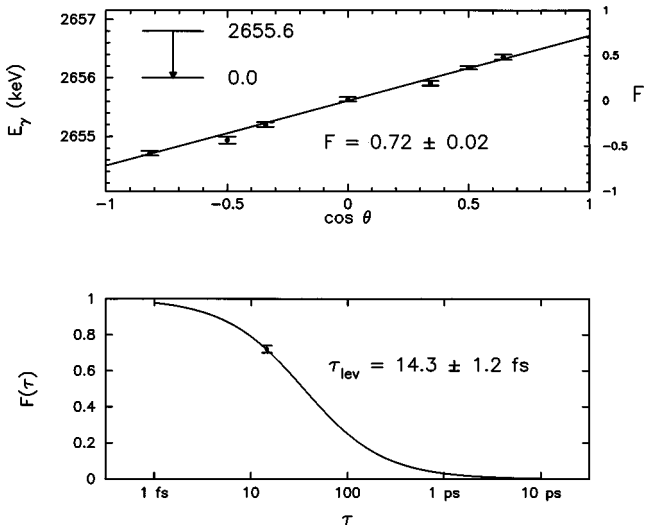

FIG. 5. Doppler-shift data for the 2655.5-keV ground-state transition. The experimental value of the Doppler-shift attentuation factor $F(\tau)$ is determined from the slope of the best-fit line. This $F(\tau)$ is then compared to theoretical values calculated using the Winterbon formalism to deduce the meanlife τ.

2655.6-keV 1^+ state. This level was recently assigned $J^\pi=(1,2)^+$ by Eckert *et al.* [9]. The excitation function of the 2655.6-keV transition from our measurements is shown in Fig. 2 and the angular distribution of the same γ ray is shown in Fig. 3. Both data sets support the $J=1$ spin assignment. Meyer *et al.* [4] report a strong 582-keV transition associated with this level. In fact, they say that the strength of this decay is approximately 30 times that of other transitions depopulating this level. The excitation function we observe for the 582-keV transition agrees with the adopted assignment of this γ ray to the 2093-keV level; we see no evidence to support a second assignment to the 2655.6-keV state.

2743.2-keV 0^+ state. This level has adopted transitions of 1182 and 2047 keV [1]. Meyer *et al.* [4] claim this level also populates the 2073 keV level via a 670-keV transition with a strength about 20 times that of the decay into the 2_1^+ state. We have a strong background line at 670 keV which accounts for most, if not all, of the strength we observe and prohibits us from confirming the assignment of Meyer *et al.* [4]. The intensity we measure for the 670-keV transition with background included is less than half that of the 2046.8-keV transition. This puts an upper limit on the 670-keV γ-ray branch of 28% which is considerably less than claimed by Meyer *et al.* [4]. Excitation function calculations are in excellent agreement with the data for the 2046.8-keV transition with the branching ratios cited in Ref. [1]. The 1182.1-keV transition is a member of a doublet, but calculations for this transition which combine strength from the 0^+ state at 2743.2 keV and the 2^+ level at 2693.0 keV are also in excellent agreement with experimental data. Clearly a 670-keV branch is rather small, if it exists.

2775.3-keV (6,4) state. This level has two adopted transitions of 682 and 1268 keV [1] with transitions near the latter energy multiply placed in the decay scheme. The 1268.1-keV transitions observed in our measurement are placed with the 2779.0- and 2829.3-keV levels. A placement of a 1268.1-

TABLE I. Levels and transition rates in ^{144}Nd. Uncertainties are in the last digit(s) except for τ. Transition rate uncertainties are from the uncertainties in the level lifetime and do not reflect uncertainties in the multipole-mixing ratio.

J^π	E_x (keV)	E_γ (keV)	Note	E_f (keV)	B %	$\tan^{-1}(\delta)$ [a]	τ (fs)	$B(E1)$ (W.u.) [l]	$B(M1)$ (W.u.) [m]	$B(E2)$ (W.u.) [n]
2^+	696.51(01)	696.51(01)	b	0	100		6510^{+340}_{-340}			17^{+1}_{-1}
4^+	1314.62(04)	618.11(04)	b	697	100		10680^{+1300}_{-1300}			19^{+3}_{-2}
3^-	1510.86(03)	197.02(06)	c	1315	3		324^{+123}_{-72}	$4.3^{+12}_{-12}E-3$		
		814.17(01)	c	697	97			$2.0^{+6}_{-5}E-3$		
2^+	1560.98(02)	864.34(03)	b, c, d	697	91	(-0.75^{+19}_{-66})	810^{+72}_{-72}		$3.0^{+3}_{-2}E-2$	20^{+2}_{-2}
		1561.14(04)		0	9					0.22^{+2}_{-2}
6^+	1791.53(05)	476.91(03)		1315	100		*			
2^+	2072.91(03)	1376.32(03)		697	72(1)	0.56^{+28}_{-25}	80^{+19}_{-14}		$7.9^{+17}_{-15}E-2$	9.4^{+20}_{-18}
		2073.11(06)		0	28(1)					1.7^{+4}_{-3}
0^+	2084.66(03)	1388.12(03)		697	100		175^{+117}_{-55}			20^{+9}_{-8}
5^-	2093.16(04)	302.31(04)	b	1792	12(1)		1200^{+1100}_{-400}	$1.3^{+6}_{-6}E-3$		
		582.34(06)		1511	10(1)					23^{+11}_{-11}
		778.52(03)		1315	78(2)			$4.9^{+24}_{-23}E-4$		
4^+	2109.87(03)	794.96(03)		1315	3(1)	-0.53^{+56}_{-41}	$577^{+\mathrm{inf}}_{-294}$		$<5.0E-3$	<1.6
		1413.44(03)		697	97(1)					<11
3^+	2178.84(02)	667.97(06)	c	1511	8		81^{+61}_{-29}	$1.2^{+7}_{-5}E-3$		
		864.34(03)	c, d	1315	59	*				
		1482.26(03)	c	697	33	0.66^{+59}_{-22}			$2.5^{+14}_{-11}E-2$	3.9^{+22}_{-17}
1^-	2186.00(02)	624.7	c	1561	0.11		21^{+3}_{-3}	$7.6^{+13}_{-10}E-5$		
		675.80(41)	c	1511	0.28					17^{+3}_{-2}
		1489.35(03)	d	697	29(1)			$1.5^{+2}_{-2}E-3$		
		2186.10(03)		0	71(1)			$1.1^{+2}_{-1}E-3$		
4^-	2204.76(06)	694.28(40)	c, e	1511	93		*			
		890.13(04)	c	1315	7					
6^+	2218.45(06)	426.92(03)		1792	100	-0.22^{+16}_{-9}	*			
4^+	2295.54(07)	734.97(05)		1561	4(2)		$996^{+\mathrm{inf}}_{-605}$			<8.7
		784.55(03)		1511	12(2)			$<23E-5$		
		980.76(04)		1315	77(2)	-0.44^{+9}_{-9}			$<5.4E-2$	<7.2
		1598.91(06)		697	7(2)					<0.31
0^+	2328.15(03)	1631.61(03)		697	100		362^{+884}_{-164}			4.4^{+36}_{-31}
2^+	2368.71(03)	1672.05(04)	f	697	84(1)	$(0.13^{+0.18}_{-0.16})$	56^{+22}_{-15}		0.10^{+4}_{-3}	0.35^{+13}_{-10}
		2368.83(04)		0	16(1)					0.70^{+26}_{-20}
5^+	2420.75(03)	202.74(03)		2219	51(1)	-0.06^{+12}_{-10}	*			
		310.82(03)		2110	34(1)	-0.03^{+6}_{-6}				
		628.64(08)		1792	15(1)	-0.75^{+40}_{-38}				
4^+	2451.78(03)	1137.02(04)		1315	77(1)	0.56^{+16}_{-40}	56^{+20}_{-14}		0.21^{+7}_{-6}	37^{+12}_{-10}
		1755.32(04)		697	23(1)					4.5^{+15}_{-12}
2^+	2527.77(02)	966.58(04)		1561	16(1)	0.09^{+16}_{-4}	58^{+11}_{-9}		$9.6^{+18}_{-15}E-2$	0.48^{+9}_{-8}
		1831.15(04)	d	697	32(1)	(0.56^{+22}_{-18})			$2.0^{+4}_{-3}E-2$	1.4^{+3}_{-2}
		2527.90(03)		0	52(1)					1.6^{+3}_{-3}
(3^+)	2564.34(02)	454.01(03)	k	2110	44(1)	-0.75^{+50}_{-47}				
		1003.44(03)	k	1561	23(1)	0.66^{+12}_{-7}				
		1053.63(08)	k	1511	8 (1)					
		1868.11(04)	g, k	697	25(1)	-0.03^{+9}_{-10}				
(3^+)	2582.30(03)	1885.76(03)		697	100	0.13^{+6}_{-4}				
2^+	2592.51(03)	1031.30(08)	g	1561	7(1)	0.56^{+44}_{-43}			$5.2^{+23}_{-21}E-3$	1.1^{+5}_{-4}
		1081.64(08)	g	1511	7(1)		280^{+185}_{-86}	$7.0^{+31}_{-28}E-5$		
		1896.01(03)		697	83(1)	0.35^{+63}_{-13}			$1.2^{+5}_{-5}E-2$	0.26^{+11}_{-10}
		2592.45(10)		0	3(1)					$1.7^{+7}_{-7}E-2$
4^+	2601.69(04)	1286.97(03)		1315	75(1)	0.31^{+32}_{-18}	189^{+179}_{-68}		$5.4^{+30}_{-26}E-2$	1.9^{+11}_{-9}
		1905.29(06)		697	25(1)					0.96^{+54}_{-47}
3^-	2606.03(03)	1094.66(06)		1511	31(1)	-1.29^{+57}_{-22}	146^{+29}_{-22}		$3.9^{+7}_{-7}E-3$	23^{+4}_{-4}
		1909.60(03)		697	69(1)			$2.4^{+4}_{-4}E-4$		
3^+	2655.04(04)	1340.42(02)	f	1315	100		*			
1^+	2655.56(03)	1958.81(06)		697	16(2)	*	$14.3^{+1.2}_{-1.2}$			
		2655.61(03)		0	84(2)				$9.96^{+91}_{-77}E-2$	
0^+	2675.60(04)	1979.06(04)		697	100		258^{+740}_{-121}			2.3^{+21}_{-17}

TABLE I. (*Continued*).

J^π	E_x (keV)	E_γ (keV)	Note	E_f (keV)	B %	$\tan^{-1}(\delta)$ [a]	τ (fs)	$B(E1)$ (W.u.) [l]	$B(M1)$ (W.u.) [m]	$B(E2)$ (W.u.) [n]
2^+	2692.96(04)	1131.81(08)	g	1561	15(1)	0.56^{+38}_{-31}			$<1.3E-2$	<2.4
		1182.06(07)	d	1511	12(3)			$<1.5E-4$		
		1378.32(07)	g	1315	52(2)		$398^{+\inf}_{-223}$			<11
		1996.35(29)	g	697	4(1)	*				
		2693.13(07)		0	17(1)					<0.12
(5,6)	2715.76(06)	924.41(09)		1792	27(1)		*			
		1401.05(06)		1315	73(1)					
2^+	2720.25(03)	2023.71(03)		697	97(1)	-0.25^{+13}_{-9}	200^{+119}_{-57}		$1.7^{+7}_{-7}E-2$	0.16^{+6}_{-6}
		2720.90(60)		0	3(1)					$1.8^{+7}_{-7}E-2$
4^+	2732.83(04)	1171.9	i	1561	3(1)					0.84^{+83}_{-70}
		1418.15(03)		1315	74(4)	0.38^{+25}_{-22}	295^{+1547}_{-147}		$2.4^{+24}_{-20}E-2$	1.1^{+11}_{-9}
		2036.41(07)		697	23(3)					0.41^{+41}_{-34}
0^+	2743.22(05)	1182.06(07)	c, d	1561	17					14^{+8}_{-6}
		2046.85(07)	c	697	83		93^{+75}_{-34}			4.5^{+26}_{-20}
(6,4)	2775.26(05)	682.10(03)		2094	100					
3^-	2778.99(03)	1217.93(16)	g	1561	12(2)		94^{+75}_{-34}	$2.5^{+14}_{-11}E-4$		
		1268.12(04)	f, g	1511	35(3)	(-0.35^{+16}_{-9})			$5.1^{+29}_{-23}E-2$	2.4^{+14}_{-11}
		1464.33(04)	g	1315	13(2)			$1.6^{+9}_{-7}E-4$		
		2082.57(07)		697	40(2)			$1.7^{+9}_{-7}E-4$		
6^+	2808.81(07)	1017.27(08)		1792	46(2)	1.26^{+19}_{-13}	$194^{+\inf}_{-130}$		$<2.0E-2$	<109
		1494.21(10)		1315	54(2)					<21
(2^+)	2829.30(03)	1268.12(04)	f	1561	17(2)	(-0.19^{+13}_{-16})	101^{+98}_{-40}		$2.6^{+17}_{-13}E-2$	$2.4^{+16}_{-12}E-1$
		1318.63(50)	g	1511	11(1)			$1.7^{+11}_{-8}E-4$		
		1515.08(05)	g, j	1315	41(5)					9.7^{+64}_{-48}
		2132.76(08)		697	31(3)	0.53^{+35}_{-28}			$7.2^{+47}_{-36}E-3$	$3.1^{+21}_{-15}E-1$
(4^+)	2834.67(03)	539.20(03)	t	2295	50(5)	(0.13^{+72}_{-22})	*			
		724.63(05)	g	2110	18(2)	0.91^{+41}_{-138}				
		1323.98(10)		1511	32(3)					
2^+	2839.53(04)	660.42(06)	g	2179	15(1)	-0.16^{+25}_{-34}			$6.5^{+52}_{-45}E-2$	2.2^{+18}_{-15}
		1524.95(24)	g	1315	6(1)		249^{+567}_{-111}			0.53^{+43}_{-37}
		2143.06(05)		697	52(1)	-0.97^{+28}_{-31}			$2.2^{+17}_{-15}E-3$	0.57^{+46}_{-40}
		2839.76(08)		0	27(1)					0.11^{+9}_{-7}
(3,2)	2868.24(05)	1357.37(04)		1511	72(1)	-0.72^{+16}_{-16}	$626^{+\inf}_{-429}$		$<2.6E-2$	<6.3
		1553.74(19)	g	1315	12(1)			$<5.8E-5$		
		2171.70(14)	g	697	16(1)			$<2.8E-5$		
(4,5)	2887.89(06)	794.96(08)		1315	100	-0.94^{+31}_{-13}	*			
		1573.04(08)		1315	100	-0.94^{+31}_{-13}	*			
2^+	2901.47(03)	722.66(09)	k	2179	10(1)	0.85^{+50}_{-44}	$194^{+\inf}_{-113}$			
		1340.42(03)	f, k	1561	24(3)	*				
		1390.34(14)	k	1511	37(1)					
		1586.47(16)	k	1315	7(1)					
		2205.13(11)	k	697	13(1)	0.85^{+41}_{-91}				
		2901.83(08)	k	0	9(1)					
$1(^+)$	2905.22(07)	1343.30(09)	h, k	1561	40(1)	-0.66^{+75}_{-72}	34^{+15}_{-10}		$9.6^{+40}_{-29}E-2$	18^{+8}_{-6}
		2905.22(03)	k	0	60(1)			$2.3^{+10}_{-7}E-2$		
$3(^+)$	2951.04(06)	841.08(06)	h, k	2110	48(1)	0.85^{+54}_{-54}	$211^{+\inf}_{-128}$		$<1.3E-1$	<141
		(877.94)	k	2073	11(1)	-0.69^{+45}_{-47}			$<8.8E-2$	<19
		2254.71(10)	k	697	41(1)	-1.13^{+22}_{-16}			$<2.5E-3$	<1.3
(2^+)	2961.76(07)	1450.91(07)	h, k	1511	79(1)			$4.7^{+42}_{-30}E-4$		
		2961.58(29)	k	0	21(1)		194^{+350}_{-91}			$8.7^{+76}_{-56}E-2$
3^-	2968.31(05)	1653.44(09)	k	1315	25(1)		35^{+73}_{-24}	$5.6^{+122}_{-38}E-4$		
		2271.86(06)	g, k	697	75(1)			$6.5^{+142}_{-44}E-4$		
1	2975.43(07)	2278.83(09)	k	697	60(1)		25^{+17}_{+11}			
		2975.54(12)	k	0	40(1)					
4^+	2980.02(06)	1665.39(06)	g, k	1315	47(1)	-0.88^{+22}_{-72}	48^{+43}_{-21}		$2.7^{+21}_{-13}E-2$	8.3^{+64}_{-39}
		2283.50(10)	k	697	53(1)					3.2^{+25}_{-15}
4^+	2986.03(04)	1671.32(02)	f, k	1315	84(8)					
		2291.03(18)	g, k	697	16(2)					
	3000.22(05)	1489.35(04)	d	1511						
		2304.50(40)	g	697						
$(4^+,3)$	3020.46(08)	1459.44(14)	k	1561	39(1)					
		2323.94(10)	k	697	61(1)					

TABLE I. (*Continued*).

J^π	E_x (keV)	E_γ (keV)	Note	E_f (keV)	B %	$\tan^{-1}(\delta)$ [a]	τ (fs)	$B(E1)$ (W.u.) [l]	$B(M1)$ (W.u.) [m]	$B(E2)$ (W.u.) [n]
	3026.29(35)	1515.08(50)	j	1511						
		1712.02(50)	h	1314						
	3029.00(12)	2332.46(12)		697	100					
(3^+)	3043.50(08)	933.69(14)	k	2110	30(1)	-0.09^{+40}_{-170}			$8.5^{+115}_{-76}E-2$	0.45^{+62}_{-40}
		1731.15(30)	g, k	1315	21(2)	0.85^{+44}_{-44}	137^{+1122}_{+79}		$4.1^{+56}_{-37}E-3$	1.0^{+14}_{-9}
		2346.62(11)	k	697	49(1)	-0.69^{+29}_{-25}			$5.2^{+71}_{-47}E-3$	0.37^{+51}_{-33}
	3048.21(09)	1733.59(08)		1315	100					
5^-	3053.45(09)	834.84(11)	k	2219	61(8)					
		1543.08(48)	g, k	1511	17(6)					
		1738.97(13)	g, k	1315	22(7)					
(5,4)	3065.08(16)	(954.7)	g	2110	20(5)					
		(970.9)	g	2094	24(6)					
		1750.46(16)		1315	56(7)					
(3^+)	3070.89(07)	(997.60)	g	2073	11(1)	0.31^{+161}_{-40}			$8.4^{+39}_{-27}E-2$	5.0^{+23}_{-16}
		2374.35(07)		697	89(1)	0.38^{+12}_{-13}	38^{+18}_{-12}		$4.8^{+22}_{-15}E-2$	$7.8^{+36}_{-25}E-1$
2^+	3100.27(09)	1027.49(18)		2073	23(1)	0.60^{+60}_{-56}	98^{+152}_{-45}		$4.7^{+40}_{-28}E-2$	12^{+10}_{-7}
		2403.66(11)		697	57(1)	0.60^{+44}_{-47}			$9.1^{+77}_{-55}E-3$	0.42^{+36}_{-26}
		3100.50(35)	g	0	20(1)					$1.3^{+11}_{-8}E-2$
	3104.55(12)	2408.01(12)	h	697						
(3,2)	3126.50(09)	947.50(14)	g	2179	20(3)					
		1565.35(20)	g	1561	25(4)					
		1811.77(34)		1315	12(3)					
		2430.19(11)		697	43(4)					
	3132.74(50)	1039.83(50)		2093	100					
	3136.44(27)	1043.95(50)		2093	50(9)					
		1821.66(31)	h	1315	50(9)					
	3145.81(06)	1636.10(50)		1511						
		1831.15(04)	d	1315						
		2450.10(35)	g	697						
$1(^+)$	3169.74(13)	1608.73(16)	h	1561	71(2)					
		3169.81(24)		0	29(2)					
(1,2)	3185.54(12)	1006.06(20)		2179	25(4)					
		2489.04(19)		697	63(4)					
		3186.45(25)		0	12(2)					
(3)	3202.55(29)	2506.01(29)		697	100					
(1,2)	3213.96(52)	3213.96(52)		0						
	3222.22(18)	1661.24(18)		1561						
(1,2)	3245.50(50)	3245.50(50)		0						
	3252.30(50)	1691.32(50)		1561						

[a] In situations where χ^2 vs δ plots yield two equivalent solutions for the mixing ratio, the lower $\tan^{-1}(\delta)$ value has been used. The alternate solution leads to much larger $B(E2)$ rates and smaller $B(M1)$ rates. The mixing ratio and B(XL)'s presented are those of the first spin listed when the spin of the initial state is not definite. Angular distributions of $1^+ \rightarrow 2^+$ transitions are not sufficiently sensitive to the mixing ratio to allow a reliable determination. Lifetimes >1ps are too long to be measured using DSAM and are denoted by an asterisk, as are undeterminable mixing ratios. Parentheses around mixing ratios indicate the transition is multiply placed. Parentheses around E_γ indicate a tentative placement.

[b] Mean lifetimes for the 696.5- and 1314.6-keV states are taken from Ref. [1] and for the 1560.9- and 2093.2-keV states from Ref. [8].

[c] Branching ratios taken from Ref. [1].

[d] Transition multiply placed in agreement with Ref. [1].

[e] Not resolved from the 696.5 keV first-excited state transition. Branching ratio from Ref. [1] and parity from [8].

[f] Transition multiply placed; strength divided using Ref. [26].

[g] New transition.

[h] New level.

[i] The presence of two levels with nearly identical decays listed in Ref. [1] is not verified in this work. Branching ratios and J^π listed are based on a single level.

[j] Transition multiply placed with the strength divided using excitation functions.

[k] Branching ratios reflect observed γ-ray intensities obtained from the angular distributions for the transitions listed; excitation function calculations, however, indicate one or more transitions are missing or that a statistical model does not well represent the data at this energy.

[l] $B(E1)_{\text{W.u.}} = 1.7702\, e^2\ \text{fm}^2$.

[m] $B(M1)_{\text{W.u.}} = 1.7905 \mu_N^2$.

[n] $B(E2)_{\text{W.u.}} = 44.796\, e^2\ \text{fm}^4$.

TABLE II. Comparison of experimental $B(E2;2^+\rightarrow 0_1^+)$ rates for 2^+ states in ^{144}Nd and ^{142}Ce from inelastic neutron scattering (INS), electron scattering, and Coulomb excitation (CE). Transition rates are listed in Weisskopf units.

State	^{144}Nd (INS)	^{142}Ce (INS)	^{144}Nd(e,e') [a]	^{142}Ce(e,e') [b]	^{144}Nd (CE) [c]	^{142}Ce (CE) [c]
2_1^+	–	–	20.5(20)	20.5(10)	21.9(2)	21.8(18)
2_2^+	0.22(1)	>0.023	–	–	0.133(27)	<0.364
2_3^+	1.7(4)	2.5(2)	2.8(2)	2.8(1)	2.90(71)	3.18(50)
2_4^+	0.70(26)	2.6(4)	1.1(1)	2.1(2)		
2_5^+	1.6(3)	0.27(16) [d]	1.5(2)	2.3(2) [d]		

[a]Reference [7].
[b]Reference [32].
[c]Reference [3].
[d]Interpretation of measured transition rates in ^{142}Ce is complicated by a doublet at this energy.

keV transition with the 2775.3-keV level would be well outside our energy uncertainty, and our placements are consistent with γ-γ coincidence measurements of Ref. [26]. The 682.1-keV transition has an angular distribution which leads to a $J=(6,4)$ preference. Excitation functions are in agreement with a $J=6$ assignment, provided it is a 100% decay branch.

2779.0-keV 3^- state. Three new transitions of 1217.9, 1268.1, and 1464.4 keV are observed for this level. The 1268.1-keV transition is also assigned to the 2829.3-keV level. It was previously assigned to the 2775.3-keV level by Snelling and Hamilton [26] as discussed above. The strength of the 1268.1-keV transition was divided between the 2779.0- and 2829.3-keV levels using the strength division of Ref. [26]. (We assumed their placement was incorrect but not their distribution of strength.) The angular distributions and the excitation functions are all consistent with $J^\pi=3^-$.

2829.3-keV 2^+ state. See the 2775.3- and 2779.0-keV level discussion of the 1268.1-keV transition. We observe a doublet at 1515 keV. One of the lines clearly belongs to the 2829.3-keV level and is a new assignment; the other transition is adopted and belongs to the 3026.3-keV level.

2839.5 keV 2^+ state. This level was recently reported as having an uncertain spin of (1) by Eckert *et al.* [9]. We observe a ground-state decay which has an angular distribution highly characteristic of $E2$ radiation, as shown in Fig. 3. All other transitions from this level have angular distributions consistent with a spin 2 assignment.

TABLE III. Absolute transition rates for negative parity states in ^{144}Nd from inelastic neutron scattering (INS) and from the γ-ray induced Doppler broadening technique (GRID). Transition rates are also given from nuclear resonance fluorescence measurements for decays of the 1_1^- level. Uncertainties are in the last digits.

Initial state	Final state	Transition energy (keV)	Multipolarity	$B(EL)$ (INS) W.u.	$B(EL)$ (GRID) [a] W.u.
3_1^-	2_1^+	814.2	$E1$	$1.9(5)\times10^{-3}$	$1.0(1)\times10^{-3}$
	4_1^+	197.1	$E1$	$4.4(13)\times10^{-3}$	$1.3(1)\times10^{-3}$
1_1^-	0_1^+	2186.0	$E1$	$1.1(2)\times10^{-3}$	$1.4(2)\times10^{-3}$ [b]
					$1.6(2)\times10^{-3}$ [e]
					$1.8(1)\times10^{-3}$ [f]
	2_1^+	1489.3	$E1$	$1.4(3)\times10^{-3}$	$1.8(5)\times10^{-3}$ [b]
					$2.1(3)\times10^{-3}$ [e]
					$2.3(4)\times10^{-3}$ [f]
	3_1^-	675.8	$E2$	17(3) [c]	20(5)
	2_2^+	624.7	$E1$	$7.5(14)\times10^{-5}$ [c]	$1.0(3)\times10^{-4}$
5_1^-	4_1^+	778.6	$E1$	$4.8(24)\times10^{-4}$ [d]	$5(2)\times10^{-4}$
	3_1^-	582.4	$E2$	23(11) [d]	$20(+12,-10)$
	6_1^+	302.4	$E1$	$1.3(6)\times10^{-3}$ [d]	$8(4)\times10^{-4}$

[a]Reference [8].
[b]Recalculated using the branching ratio correction discussed in Ref. [9].
[c]Branching ratios from Ref. [1].
[d]Mean lifetime from Ref. [8].
[e]From Ref. [38].
[f]From Ref. [9].

3100.3-keV 2^+ state. This level has an adopted $J=(2,3,4)$. The adopted transition of 1787.0-keV is not observed in this measurement; however, a ground-state transition is observed with an angular distribution that indicates $J^\pi=2^+$ for this level.

Previously adopted levels not observed in this experiment are the 2270-, 2321-, 2399-, 2447-, 2508-, 2612-, 2613-, 2681-, 2709-, 2768-, 2803-, 2842-, 2876-, 2903-, 2945-, 2964-, 2972-, 3031-, 3056-, 3084-, 3161-, and 3178-keV states. A few of these unobserved levels have spins >6 and are generally not expected to be observed with the $(n,n'\gamma)$ reaction.

We were unable to confirm transitions listed in Ref. [1] for the following levels whose decays we did detect. The levels and (transition energies in keV) are 2084.7 keV (574), 2295.5 keV (201.6), 2582.3 keV (1268), 2775.3 keV (1268), 2980.0 keV (906,2979), 3100.3 keV (1787), and 3202.6 keV (1023).

IV. MIXED-SYMMETRY EXCITATIONS

A. Overview

Mixed-symmetry excitations (MS) were first investigated experimentally in the $N=84$ isotones ^{140}Ba, ^{142}Ce, and ^{144}Nd by Hamilton *et al.* [10]. The focus of their investigation was the 2_3^+ level in each of these nuclei since this state could not be accommodated within the IBM-1 [10]. Using their measured branching ratios and $E2/M1$ multipole-mixing ratios, along with IBM-2 calculations, they deduced that the 2_3^+ state in each of these nuclei exhibited MS properties consistent with those predicted in the U(5) limit of the IBM-2 by Iachello [17]. Furthermore, the MS strength was reported to be isolated in each of these levels. The predicted properties of these low-lying MS states in spherical nuclei are small $E2/M1$ multipole-mixing ratios ($|\delta|\lesssim 0.3$), $B(E2;0_1^+\rightarrow 2_{MS}^+)\approx 3$ W.u., and unusually large $M1$ transition rates to the lowest symmetric 2^+ state [12,17]. Additionally, the lowest MS states in spherical nuclei are predicted to occur between 2–3 MeV and have $J^\pi=2^+$ [17]. Vermeer *et al.* [15] measured $B(E2;0_1^+\rightarrow 2_3^+)$ for ^{142}Ce via Coulomb excitation and used branching and multipole-mixing ratios from Ref. [27] to support further the identification of the 2_3^+ level as an isolated MS state in this $N=84$ isotone. This latter work was extended by Spear *et al.* [3] to include ^{144}Nd with the same conclusion, i.e., the MS strength is isolated in the the 2_3^+ state of each of these nuclei.

Fragmentation of the $M1$ mixed-symmetry mode, however, has been observed in numerous deformed nuclei [12]. In spherical nuclei, specifically in the $N=84$ isotones, fragmentation has been predicted by various models [4,13,14,28] and was recently observed in ^{142}Ce by Vanhoy *et al.* [16]. Cottle *et al.* [5] investigated excited levels in ^{144}Nd and found $B(E2;0_1^+\rightarrow 2_3^+)$ substantially lower than the 3 W.u. predicted for MS states by Iachello [17]. This led them to predict that the MS mode may be fragmented among several 2^+ levels in this nucleus. Additionally, they suggested that the MS strength is shared between the 2_3^+ state at 2072.9 keV and the 2_4^+ level at 2109.9 keV. We have determined that the 2109.9-keV state actually has $J^\pi=4^+$ in agreement with Refs. [6,7]. Fragmentation of this MS strength in ^{144}Nd, if it exists, must reside elsewhere.

Our extended data set allows us to investigate further the question of low-lying MS states in ^{144}Nd and the fragmentation of MS strength. We include below a discussion of our IBM-2 calculations completed using the code NPBOS [29] and discuss existing model calculations from Refs. [4,13,14]. We then discuss our results for positive-parity excitations and compare these results with model calculations and with analogous excitations in ^{142}Ce, emphasizing MS interpretations.

B. Model calculations

Extensive calculations for the $N=84$ isotones, ^{138}Xe-^{146}Sm, have been completed by Copnell *et al.* [13] using the IBM-2 and the PCM. We have extended their IBM-2 calculations for ^{144}Nd to include additional levels for which experimental information is now available. The same code NPBOS [29], the same IBM-2 Hamiltonian, and the same parameter set are used in our calculations as were used by Copnell *et al.* [13] with optimizations discussed below. The number of proton and neutron bosons used in all ^{144}Nd calculations was $N_\pi=4$ and $N_\nu=1$. The former value is an effective proton boson number and is probably influenced by the $Z=64$ subshell closure [13]. The following parameter set from Ref. [13] was used as a starting point in our calculations: $\epsilon=0.850$, $\kappa=-0.27$, $C_\pi^0=0.258$, $C_\pi^2=0.258$, $C_\pi^4=0.000$, $\xi_1=\xi_3=0.35$, and $\xi_2=0.1$, with $e_{\pi,\nu}=0.12$, $g_\pi=0.7$, $g_\nu=0.2$, $\chi_\pi=0.0$, and $\chi_\nu=-0.965$. These effective charges and g-factors were derived following the procedures in Refs. [30,31]. Attempts to optimize the parameter set with the newly available information resulted in little change in the wave functions or in electromagnetic transition rates, although with alterations of the proton anharmonicity parameters, $C_\pi^0=0.50$, $C_\pi^2=0.26$, and $C_\pi^4=-0.27$, the placements of the 4_1^+ and 6_1^+ states were slightly improved. These new calculations reproduce rather well the level sequence, as can be seen in Fig. 6, and many transition rates, as shown in Table IV.

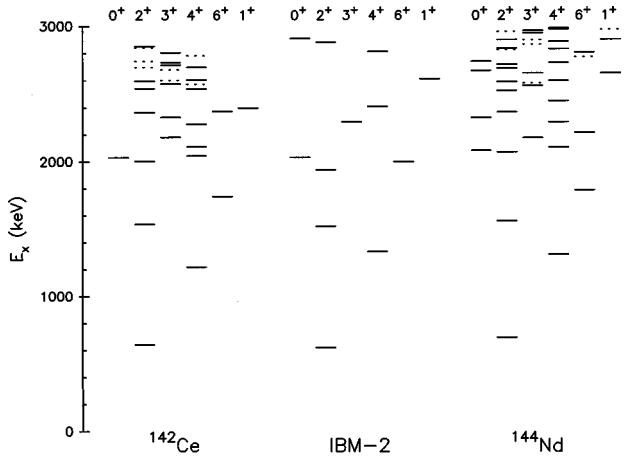

FIG. 6. Low-lying positive-parity levels of ^{142}Ce and ^{144}Nd and IBM-2 calculated levels. Dotted lines are used when level spins are uncertain. Model calculations do not well reproduce the experimental level density above 2000 keV, which indicates that these states have a more complex structure than that represented by the IBM-2.

TABLE IV. Electromagnetic properties of selected states in ^{144}Nd and ^{142}Ce with model calculations for ^{144}Nd. Transition rates listed are in Weisskopf units. Both asymmetric and symmetric uncertainties are in the last digit(s).

	^{144}Nd	^{142}Ce	IBM-2	PCM [a]	QPM [b]	QPM [c]	CVM [d]
$B(E2;2_1^+\rightarrow 0_1^+)$	17(1) [e]	21.2^{+24}_{-19}	23	17	17.0	17.0	23
$B(E3;3_1^-\rightarrow 0_1^+)$	31(1) [f]	24(2) [f]		3.66	26.7	19.7	
$B(E2;0_2^+\rightarrow 2_1^+)$	20^{+9}_{-8}	15^{+8}_{-7}	13				
$B(E2;2_2^+\rightarrow 2_1^+)$	20(2)	>19	22	12		24.6	16
$B(E2;4_1^+\rightarrow 2_1^+)$	19^{+3}_{-2}	27^{+3}_{-2}	32	15		17.9	27
$B(E2;2_2^+\rightarrow 0_1^+)$	0.22(2)	>0.023	0.49	0.1	0.35	0.446	0.223
$B(E2;2_3^+\rightarrow 0_1^+)$	1.7^{+4}_{-3}	2.5(2)	<0.02	2.2	0.67	2.46	1.56
$B(E2;2_4^+\rightarrow 0_1^+)$	0.70^{+26}_{-20}	2.6^{+4}_{-3}	<0.02		0.89		
$B(E2;2_5^+\rightarrow 0_1^+)$	1.6(3)	0.27^{+16}_{-15}	<0.02		0.98		
$B(E2;2_3^+\rightarrow 2_1^+)$	9.4^{+20}_{-18} $[2.9^{+6}_{-6}]$ [g]	2.6(3)	3.43	2		10.5	4.01
$B(E2;2_4^+\rightarrow 2_1^+)$	0.35^{+13}_{-10}	0.037^{+6}_{-5}	<0.02				
$B(E2;2_5^+\rightarrow 2_1^+)$	1.4^{+3}_{-2}	0.028^{+17}_{-15}	<0.02				
$B(M1;2_2^+\rightarrow 2_1^+)$	0.030^{+3}_{-2}	>0.012	0.012	0.017		0.067	0.0073
$B(M1;2_3^+\rightarrow 2_1^+)$	0.079^{+17}_{-15} $[0.10^{+2}_{-2}]$ [g]	0.13(1)	0.030	0.0977		0.201	0.090
$B(M1;2_4^+\rightarrow 2_1^+)$	0.10^{+4}_{-3}	0.20(3)	<0.0001				
$B(M1;2_5^+\rightarrow 2_1^+)$	0.020^{+4}_{-3}	0.0046(28)	0.0025				
$Q(2_1^+)(e\text{b})$	$-0.15(6)$ [f]	$-0.16(5)$ [f]					

[a]Reference [13].
[b]Reference [7].
[c]Reference [14].
[d]Reference [4].
[e]Reference [1].
[f]Reference [3].
[g]Mixing ratio from Ref. [26].

Calculations from three other models, the PCM, QPM, and CVM, are presented in the Table IV and discussed in the text. These models all contain both particle and collective features, but they treat these configurations in different ways. No new calculations have been completed using these models, rather the reader is referred to the literature for details of the models and for the specific calculations for ^{144}Nd. In particular, the calculations we have included in this work are from Copnell *et al.* for the PCM [13], Meyer *et al.* for the CVM [4], and Dinh *et al.* [14] and Perrino *et al.* for the QPM [7].

C. States with mixed-symmetry character

1. 1^+ states

The 1^+ state at 2655.6 keV state exhibits a fast $M1$ transition to the ground state. The Doppler shifts for the level are shown in Fig. 5. The experimental transition rate of $B(M1;1_1^+\rightarrow 0_1^+)=0.10(1)$ W.u. deduced for this level is only slightly larger than recent measurements of $B(M1;1_1^+\rightarrow 0_1^+)=0.061(4)$ W.u. by Eckert *et al.* [9]. The experimental value is over a factor of four larger than predicted by IBM-2 calculations even though the model predicts the wave function of the 1_1^+ level to contain 96% MS components.

We also observe the decay of the 2655.6-keV level into the 2_1^+ level, but the multipole-mixing ratio cannot be determined from the data. The ambiguity we observe for $\delta(1_1^+\rightarrow 2_1^+)$ is not unusual for decays from spin 1 states as the χ^2 versus $\tan^{-1}(\delta)$ plots are often very flat. In ^{142}Ce, the experimental picture is better determined. The 1_1^+ level in that nucleus exhibits $M1$ decays in very good agreement with IBM-2 calculations [16], although calculated $E2$ decay strengths into the 2_1^+ and 2_2^+ states are essentially reversed from the experimental values. Of the models considered, transition rates for the 1^+ decays are available only for the IBM-2.

2. 2^+ states

Experimental transition rates for the five lowest 2^+ states in both ^{144}Nd and ^{142}Ce are given in Table IV along with theoretical calculations for ^{144}Nd from the PCM [13], the CVM [4], the QPM [7,14], and the IBM-2. The distributions of $B(M1;2_x^+\rightarrow 2_1^+)$ and $B(E2;2_x^+\rightarrow 0_1^+)$ for $x=(2-6)$ are shown in Fig. 7 for ^{144}Nd and ^{142}Ce.

Evaluation of MS strength in 2^+ states in ^{144}Nd depends strongly on the value of the multipole-mixing ratios for decays to the 2_1^+ symmetric state. In Table V, we list our $E2/M1$ multipole-mixing ratios along with values from Snel-

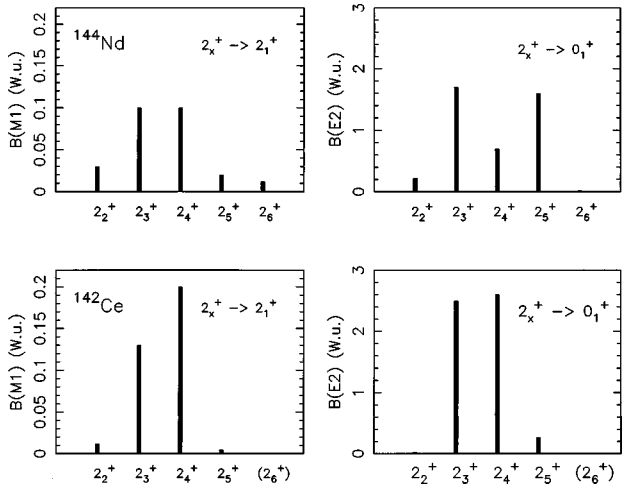

FIG. 7. Magnetic-dipole and electric-quadrupole transition rates for decays from 2_x^+ states into the 2_1^+ and 0_1^+ levels in ^{144}Nd and ^{142}Ce are shown in the top two panels and bottom two panels, respectively.

ling and Hamilton [26] and Al-Janabi *et al.* [25]. Our evaluation is complicated by doublets at the energies of the decays into the 2_1^+ state for the $2_2^+, 2_4^+$ and the 2_5^+ levels. In each case, the other member of the doublet belongs to a higher-energy level and is considerably weaker. Our values are in good agreement with those of Ref. [26] and also for some transitions with Al-Janabi *et al.* [25], as can be seen in Table V. Transition rates for decays from the 2_3^+ state are listed in Table IV and have been calculated using both our mixing ratio and that of Ref. [26], which is consistent with ours within the uncertainties and is at the upper limit of $\delta \lesssim 0.3$ predicted for MS states [12]; it is also the value used in our discussion and in Fig. 7. All other transition rates are calculated using our δ's. Only the multipole-mixing ratios for the 2_3^+ and 2_4^+ states in ^{144}Nd lie within the limits indicative of MS strength in spherical nuclei [12], as the others have too large an $E2$ component. The same is also true of the 2_5^+ state in the $N=84$ isotone ^{142}Ce [16].

Examination of Fig. 7 reveals that most of the $M1$ decay strength from low-lying 2^+ states in ^{144}Nd lies in the 2_3^+ and 2_4^+ levels, although the rates are only reduced by a factor of 3-6 in the $2_2^+, 2_5^+$ and 2_6^+ states. The $M1$ strength in ^{142}Ce is much more concentrated in the 2_3^+ and 2_4^+ levels. Lipas [12] reports that values of $B(M1; 2^+_{\rm MS} \rightarrow 2_1^+)$ between 0.06 to 0.28 W.u. are typically used to identify MS states. This again points to the 2_3^+ and 2_4^+ levels as the best candidates for MS states in these two nuclei. Lipas also reports that within the U(5) limit of the IBM-2 the summed $M1$ strength for $2^+_{\rm MS} \rightarrow 2_1^+$ decays should be about $0.23\mu_N^2$. This prediction compares well with our observed values of $0.36\mu_N^2$ for ^{144}Nd and $0.59\mu_N^2$ for ^{142}Ce for just these two levels.

TABLE V. Multipole-mixing ratio comparison for 2^+ states in ^{144}Nd. Uncertainties are in the last digit(s).

Transition	This work	Ref. [26]	Ref. [25]
$\delta(2_2^+ \rightarrow 2_1^+)$	-0.93^{+30}_{-523}	$-(1.13^{+22}_{-15})$	-0.73(8)
$\delta(2_3^+ \rightarrow 2_1^+)$	0.63^{+49}_{-31}	0.31^{+11}_{-9}	0.13(7) 1.70(30)
$\delta(2_4^+ \rightarrow 2_1^+)$	0.13^{+19}_{-16}	0.17(8)	0.15^{+9}_{-6} 1.57(27)
$\delta(2_5^+ \rightarrow 2_1^+)$	0.63^{+36}_{-23}		0.07^{+6}_{-8} 1.86^{+42}_{-34}

A final signature of MS strength in spherical nuclei is $B(E2; 0_1^+ \rightarrow 2^+_{\rm MS}) \approx 3$ W.u. [17]. In ^{142}Ce, the $E2$ decay strength to ground is clearly isolated in the 2_3^+ and 2_4^+ levels, while in ^{144}Nd, the strength is spread into the 2_5^+ state and to a lesser extent into the 2_2^+ state, as can be seen in Fig. 7. The summed $E2$ strengths for the ground-state decays of 2.4 and 5.1 W.u. for just these two levels in ^{144}Nd and ^{142}Ce, respectively, are slightly larger than Iachello's predictions for the lowest $2^+_{\rm MS}$ levels in U(5) nuclei [17].

Our experimental results show that in these two $N=84$ nuclei, both the 2_3^+ and 2_4^+ states exhibit properties consistently predicted for MS excitations in spherical nuclei, even though they are split by over 300 keV. There is also some evidence of spreading of a little of this strength into the 2_2^+ and 2_5^+ levels.

The overlap between IBM-2 wave functions and the harmonic U(5) wave functions has been calculated in order to evaluate the symmetric versus MS character of the levels in ^{144}Nd; the results of these calculations for ^{142}Ce have been given previously in Table III of Ref. [16]. There is essentially no difference in the overlap integrals for ^{144}Nd so the reader is referred to that work for details of the calculation. Specific overlaps are discussed below for states of interest in ^{144}Nd. The IBM-2 2_1^+ state is highly symmetric as its wave function is composed predominantly (78%) of the $2_1^+(d)$ symmetric boson. The $E2$ decay of this state is reproduced rather well by the model. The second, third, and fifth IBM-2 2^+ states all have a significant one d-boson 2_M(d) component, with the 2_3^+ state receiving the largest contribution of $\approx 55\%$. The two d-boson $2_M(d^2)$ strength is split between the fourth and fifth 2^+ states. The MS component in the calculated IBM-2 2_4^+ and 2_5^+ states is not revealed through large $M1$ decay rates into the symmetric 2_1^+ level; in fact, the $M1$ rates are very small compared to the same rate from the 2_2^+ and 2_3^+ levels. The IBM-2 $M1$ decay rates are in rather good agreement with the data except for the 2_4^+ state, although all are consistently a bit low, as can be seen in Table IV.

The $E2$ decay rates of the $2_3^+, 2_4^+$, and 2_5^+ levels to the ground state are all underpredicted by the model, as are the decays of the 2_4^+ and 2_5^+ states to the 2_1^+ level. The model does do well with $E2$ transitions from the 2_2^+ state and the $2_3^+ \rightarrow 2_2^+$ decay. The total $E2$ strength of 94 W.u. predicted by the IBM-2 for these 2^+ levels, however, is in rather good agreement with the total experimental $E2$ value of 85 W.u. There appears to be an $E2$ strength distribution problem in the model for these ^{144}Nd levels. We were unable to adjust IBM-2 model parameters to correct any of the above problems.

Dinh *et al.* [14] use the QPM to examine the three lowest 2^+ states in several $N=84$ isotones and to investigate MS strength distributions in these levels. Results of their calculations are given in the last column of Table IV; the overall agreement with our experimental data for ^{144}Nd is quite good. With respect to the main component of the QPM wave function, they find the 2_1^+ and 2_2^+ states to be symmetric collective excitations, with the lowest 2^+ state being predominantly a single-phonon excitation and the 2_2^+ level a two-phonon excitation. They also find that MS strength is shared between the 2_2^+ and 2_3^+ states with the 2_3^+ level having about a 50% MS component. The model actually predicts similar $M1$ rates from these two 2^+ levels, even though the 2_3^+ state has a much larger MS component. Unfortunately, no results from these QPM calculations are given for any higher-lying 2^+ states. Perrino *et al.* [7] list QPM calculations for $B(E2;0_1^+\rightarrow 2^+)$ rates for additional 2^+ levels which they compare to their electron-scattering data. These calculations are presented in the seventh column of Table IV and are found to agree within a factor of two with our data for the limited number of transitions listed. There is, however, some disparity between the two sets of QPM calculations, e.g., $B(E2;2_3^+\rightarrow 0_1^+)$ is almost a factor of four greater in the calculations by Dinh *et al.* [14] than in those by Perrino *et al.* [7].

The PCM calculations for ^{144}Nd by Copnell *et al.* [13] are in good agreement with most experimental transition rates. Decay of the symmetric two-phonon 2_2^+ state into the first excited state is, however, significantly underestimated, as is the decay of the 4_1^+ . The $B(E3)$ decay rate of the 3_1^- state is also much too low. Wave functions from the PCM calculations are presented in Ref. [13] for ^{144}Nd. It seems the model underpredicts the collectivity of some of the levels, e.g., the 2_2^+ state is not predicted to have significant two-phonon character in the model.

The CVM does very well with most decays, especially the ground-state decays of the 2^+ levels [4]. This model, like the QPM, predicts that the MS strength is spread between the 2_2^+ and 2_3^+ levels. The CVM, however, predicts a much bigger difference in the $M1$ decay rates for these two levels into the 2_1^+ than does the QPM or than is observed experimentally.

Comparisons of the experimental data for ^{144}Nd and ^{142}Ce reveal that the distribution of ground-state $E2$ strength differs in these two nuclei. Examination of the transition charge densities of ^{144}Nd (Fig. 7 in Ref. [7]) and ^{142}Ce (Fig. 3 in Ref. [32]), shows nearly identical structure for the first three 2^+ states. This is supported somewhat by the data, although for ^{142}Ce only a lower limit is given for $B(E2;2_2^+\rightarrow 0_1^+)$. The 2_4^+ state exhibits less collectivity or surface peaking in ^{142}Ce than does the same level in ^{144}Nd, while the 2_5^+ state displays the opposite effect; however, the 2_4^+ ground-state decay strength is clearly larger in ^{142}Ce. This is reversed from the direction expected unless one focuses on a hole interpretation, since ^{144}Nd has two more proton particles than ^{142}Ce with respect to $Z=50$ but two less proton holes with respect to the $Z=64$ proton subshell closure.

3. 3^+ states

The $3_1^+\rightarrow 2_1^+$ transition in ^{144}Nd exhibits rather strong $M1$ and $E2$ rates. The rates observed for both of these transitions are larger than observed in ^{142}Ce or predicted by our IBM-2 calculations for the $3_{\rm MS}^+$ state in ^{144}Nd. The IBM-2 calculations indicate that the lowest $3_m^+(d^2)$ strength is split between the first and second 3^+ states. Manifestations of this split are small $M1$ transitions and sizeable $E2$ transitions into the 2_2^+ and 4_1^+ states. In ^{142}Ce, this is essentially what is observed, although the magnitudes of the measured $E2$ transition rates are not in good agreement with the IBM-2 predictions. Not enough experimental information is available to evaluate the fragmentation of 3^+ MS strength in ^{144}Nd. It is interesting that strong $M1$ decays are not predicted for these 3^+ levels, even though the IBM-2 calculations reveal that the wave functions for these levels are predominantly of MS character. Calculations for 3^+ levels were not listed from the other models.

V. MULTIPHONON EXCITATIONS

1. Quadrupole-octupole coupled structures

Quadrupole-octupole coupled (QOC) states have been investigated rather extensively in ^{144}Nd [6,8,9,33–35]. These negative-parity states with $J=(1-5)$ arise from the coupling of the quadrupole and octupole vibrational modes and should have energies near the sum of $E(2_1^+)$ and $E(3_1^-)$, which is ≈ 2200 keV in ^{144}Nd. These states are further characterized by their decay properties, since $E3$ transitions from the QOC states to the 2_1^+ state and $E2$ transitions into the 3_1^- level should have $B(E3)$ and $B(E2)$ values of the same strength as $B(E3;3_1^-\rightarrow 0_1^+)$ and $B(E2;2_1^+\rightarrow 0_1^+)$, respectively [8]. Often, however, the decays are dominated by rather strong $E1$ transitions, e.g., $B(E1;1_1^-\rightarrow 0_1^+)\simeq 10^{-3}$ W.u. [8,36]. Previous evaluations of QOC states in ^{144}Nd are discussed below, and new information on these states gleaned from this $(n,n'\gamma)$ investigation is presented. Quadrupole-octupole candidates and their associated transition rates are listed in Table VI. Similar values found for ^{142}Ce are included for comparison [16]. Many of the transition rates measured by Robinson *et al.* [8] are listed in Table III.

QOC 1^- state. The 1^- level at 2186.0 keV was originally identified as a member of the QOC quintuplet based on energy considerations alone [33,35,37]. Decay properties of this state are listed in Table III as determined in this measurement, as well as from Refs. [8,9,38]; all values are in excellent agreement. The observed $E1$ decays into the 0_1^+ and 2_1^+ levels and the $E2$ decay into the 3_1^- state are consistent with predicted QOC-state properties [8,9,35]. The 1^- QOC candidate in ^{142}Ce was observed to have similar decay properties and lies at 2188 keV [16]. Recent transition rate calculations by Tsoneva *et al.* [39] using the QPM model indicate the 1_1^- level in both ^{142}Ce and ^{144}Nd consists of a large portion of the two-phonon quadrupole-octupole component.

QOC 2^- state. The 2^- member of the QOC quintuplet remains elusive. Pignanelli *et al.* [6] see no clear indication of the 2^- state which they clearly observed in the Mo, Pd, and Cd isotopes [40]. They assert that this may be an indication that both $2^+\otimes 2^+$ and $2^+\otimes 3^-$ two-phonon states are largely fragmented in this nucleus; this assertion is supported by their QPM calculations. Calculations by Vogel and Koc-

TABLE VI. Absolute transition rates for QOC state candidates in ^{144}Nd and ^{142}Ce and for the 2_1^+ and 3_1^- levels.

	^{144}Nd					^{142}Ce				
Initial state	Level energy (keV)	Final state	Transition energy (keV)	Multi-polarity	$B(XL)$ (W.u.)	Level energy (keV)	Final state	Transition energy (keV)	Multi-polarity	$B(XL)$ (W.u.)
2_1^+	696	0_1^+	696.5	$E2$	17(1) [a]	641	0_1^+	641.3	$E2$	21(2)
3_1^-	1511	2_1^+	814.2	$E1$	2.0^{+6}_{-5} x 10^{-3}	1653	2_1^+	1011.7	$E1$	$<1.2\times10^{-4}$
		4_1^+	197.1	$E1$	$4.3(12)\times10^{-3}$		4_1^+	433.2	$E1$	$<2.2\times10^{-4}$
1_1^-	2186	0_1^+	2186.0	$E1$	$1.1^{+2}_{-1}\times10^{-3}$	2188	0_1^+	2187.4	$E1$	$1.2(3)\times10^{-3}$
		2_1^+	1489.3	$E1$	$1.5(2)\times10^{-3}$		2_1^+	1546.3	$E1$	$2.4(5)\times10^{-3}$
		3_1^-	675.8	$E2$	17^{+3}_{-2} [b]		3_1^-	(534)	$E2$	<79
		2_2^+	624.7	$E1$	$7.6^{+13}_{-10}\times10^{-5}$ [b]					
2^-						2728	2_1^+	2086.6	$E1$	$4.3(22)\times10^{-5}$ [d]
							2_2^+	1191.6	$E1$	$2.6(13)\times10^{-4}$ [d]
							3_1^-	1074.9	$M1$	$1.5(8)\times10^{-3}$ [d]
									$E2$	3.0(2) [d]
3^-	2779	2_1^+	2082.5	$E1$	$1.7^{+9}_{-7}\times10^{-4}$	2768	2_1^+	2126.5	$E1$	$2.8^{+8}_{-7}\times10^{-4}$
		4_1^+	1464.4	$E1$	$1.6^{+9}_{-7}\times10^{-4}$		2_2^+	1231.5	$E1$	$5.3^{+15}_{-13}\times10^{-4}$
		3_1^-	1268.1	$M1$	$5.1^{+29}_{-23}\times10^{-2}$ [e]		3_1^-	1115.0	$E2$	
				$E2$	2.4^{+14}_{-11} [e]					
		2_2^+	1217.9	$E1$	$2.5^{+14}_{-11}\times10^{-4}$					
4^-	2204	4_1^+	890.1			2384	4_1^+	1165.3	$E1$	$4.2^{+40}_{-26}\times10^{-4}$
		3_1^-	694.0				3_1^-	731.5	$M1$	0.44^{+38}_{-25}
									$E2$	$3.3^{+29}_{-19}\times10^{2}$
							3_1^+	202.3	$E1$	$2.5^{+21}_{-14}\times10^{-2}$
5_1^-	2093	4_1^+	778.6	$E1$	$4.9(24)\times10^{-4}$ [c]	2125	4_1^+	905.6	$E1$	$<6.6\times10^{-4}$
		3_1^-	582.4	$E2$	23(11) [c]		3_1^-	471	$E2$	<138
		6_1^+	302.4	$E1$	$1.3(6)\times10^{-3}$ [c]		6_1^+	381.8	$E1$	$<9.8\times10^{-4}$

[a]Mean lifetime from Ref. [1].
[b]Branching ratios from Ref. [1].
[c]Mean lifetime from Ref. [8].
[d]Tentative 2^- assignment [16].
[e]Ambiguous mixing ratio because of the doublet nature of the 1268-keV transition.

bach [34] using Hartree-Fock methods indicate that the 2^- QOC state is pushed well above the $2_1^+ + 3_1^-$ sum by anharmonicities. Considering levels observed in this measurement which decay into both the 2_1^+ and 3_1^- states, only one level at 3000.2 keV is not excluded by other unlikely 2^- decay patterns. More experimental information is needed before a definite assignment can be made. In ^{142}Ce, a 2^- candidate was proposed at 2728 keV based on decay characteristics; however, the spin of that level is not definite [16].

QOC 3^- state. Calculations by Vogel and Kocbach [34] predict the 3^- QOC state to lie above 3 MeV and to have an enhanced $E3$ decay to the ground state. Robinson *et al.* [8] propose the 2779.0-keV level as the 3^- candidate since a rather large $B(E3)=7.3$ W.u. is observed from this level to ground [6]; however, this assessment is made without absolute transition rates into the 2_1^+ and 3_1^- one-phonon states. Our measurements further support the QOC nature of the 3^- at 2779.0-keV. We observe decays into both the 2_1^+ and 3_1^- states, and experimental absolute transition rates given in Table VI are consistent with a QOC description for this level.

Robinson *et al.* [8] report that the QOC strength may be fragmented between several 3^- states above 2.6 MeV. This fragmentation is supported by the decay patterns and absolute transition rates of other 3^- levels. The 2606.0-keV level, for example, has a considerably stronger $E2$ decay into the 3_1^- state and a rather strong $E1$ decay into the 2_1^+ level; however, no strong $E3$ decay to the ground state has been observed for this level. In a true harmonic picture, this level actually appears to be the better candidate since no $\Delta n=2$ decays are observed, where n is the quadrupole-phonon number.

Other states which do not have definite spin and parity assignments but exhibit some of the desired decay patterns include the 2564.3-, 2868.2-, and 3000.2-keV levels, as can be seen in Table I. A level at 2768 keV was proposed as the

3^- QOC candidate in ^{142}Ce; however, the spin assignment of the state remains indefinite.

QOC 4^- state. The 2204.8-keV level has been identified as the 4^- QOC candidate by Robinson *et al.*, although the decay characteristics of this level are not completely consistent with a QOC interpretation. No new information was obtained for this level. The 4^- candidate in ^{142}Ce is located at 2384 keV [16].

QOC 5^- state. The 5_1^- level at 2093.2-keV has been proposed as a member of the QOC quintuplet [33,37]. Direct excitation investigations of this state by Cottle *et al.* [41] indicate that single-step processes contribute extensively in the excitation of this level, which suggests this state has large $2qp$ structure. Robinson *et al.* [8] observed strong decays of this level into both the 2_1^+ and 3_1^-, which led them to propose that this level has about equal contributions of QOC and $2qp$ character in its wave function. In fact, they contend that the mixing of $2qp$ and QOC configurations may explain why the level is observed a few hundred keV lower than calculated by Vogel and Kocbach [34]. Recent investigations of negative-parity states in ^{144}Nd by Jewell *et al.* [42] found this level to be well described by a wave function which is composed of 40–50% $2_1^+ \otimes 3_1^-$ and 50–60% is the $2qp$ configuration of $\nu(f_{7/2}, i_{13/2})$. Our measurements are in excellent agreement with those of Ref. [8].

2. Two-quadrupole phonon structures

The ratio $E_x(4_1^+)/E_x(2_1^+)=1.89$, the small quadrupole moment of the first excited state $Q(2_1^+)=-0.15(6)$ eb [3], and the $E2$ transition rates for decays of the $0_2^+, 2_2^+$, and 4_1^+ states into the 2_1^+ are all indicative of spherical vibrational character. The rather large energy separation between these three states, however, suggests that the anharmonicities are quite large. Additionally, the $B(E2)$ values for decays of these three levels into the 2_1^+ state are only about half of the harmonic value which, as was suggested by Pignanelli *et al.* [6], may indicate a large fragmentation of two-phonon strength in this nucleus. Comparisons of the behavior of these levels with IBM calculations led Gupta [43] to conclude that the vibrational character of these excitations is not fully developed from their more particlelike behavior in the $N=82$ isotones. The $2qp$ versus vibrational nature of the 4_1^+ level has been investigated extensively by Cottle *et al.* [5] and is discussed below. The triplet of states $(0^+, 2^+, 4^+)$ predicted from the coupling of two quadrupole phonons $(2Q)$ in a simple vibrational picture is expected to occur at twice the excitation energy of the 2_1^+; these states have long been identified in ^{144}Nd [43]. Members of this multiplet are described below only in relation to new information obtained in this work. Both experimental and theoretical transition rates discussed below are listed in Table IV.

$2Q$ 0^+ state. The first observed 0^+ state lies at 2084.7 keV and is well above twice the energy of the 2_1^+ quadrupole phonon. It remains the best candidate for the 0^+ member of the two-phonon triplet as it has a rather large $E2$ decay into the 2_1^+ state. The experimental $B(E2;0_2^+ \rightarrow 2_1^+) = 20^{+9}_{-8}$ W.u. is larger than predicted by our IBM-2 calculations, which indicate that the wave function for this state is composed of $\approx 64\%$ two-phonon components. There appears to be a distribution problem rather than a lack of overall strength for the two-phonon states in this model, since the total $E2$ decay strength from the two-phonon candidates is ≈ 69 W.u., while the IBM-2 predicts 67 W.u. for the same decays.

The PCM 0_2^+ has almost no overlap with the IBM-2 0_2^+. Copnell *et al.* [13] comment that because of this and the better overall agreement of the PCM with experiment that the experimental 0_2^+ must lie outside the IBM-2 model space. This statement is not completely supported by our data. Unfortunately, Copnell *et al.* do not list decay rates from their PCM calculations for 0^+ states. The PCM results are consistently low for all transitions from members of the two-phonon multiplet, even for the ground-state decay of the 2_2^+ state. This suggests that both the one-phonon and two-phonon strengths in this model are not sufficiently large to describe the experimental situation. The QPM actually shows better overall agreement with experiment for the 2_2^+ and 4_1^+ decays, but again, no transition rates are given for 0^+ states in Refs. [7,14]. No transition rates are given for 0^+ levels in CVM calculations [4].

$2Q$ 2^+state. The 2_2^+ level at 1561.0 keV is the best candidate for the 2^+ member of the $2Q$ triplet. The IBM-2 calculations do rather well in describing $E2$ decay rates from this state into both the 2_1^+ and 0_1^+ levels, although the latter calculation is too high and the $M1$ decay into the 2_1^+ state is too low by a factor of about 2. The PCM underpredicts both of these decays which, as discussed for the 0_2^+ level, indicates that neither the one- or two-phonon strengths are adequate for these levels.

The QPM calculations of Dinh *et al.* [14] give results similar to the IBM-2 for both $E2$ decays but overpredict the $M1$ decay. The CVM [4] does very well with the ground-state decay of the 2_2^+ level but shows mixed results for other decays.

$2Q$ 4^+ state. The excitation energy of the 4_1^+ state at 1314.6 keV is very close to the harmonic value of twice the energy of the 2_1^+ level. Its $E2$ decay rate into the 2_1^+ level is also suggestive of strong two-phonon character, although the same decay in ^{142}Ce is 8 W.u. greater [16]. Both the PCM and QPM do a considerably better job reproducing the decay rate for this level than does the IBM-2 or the CVM. This is exactly opposite of what is seen in ^{142}Ce. In that nucleus, it appears the collective, or two-phonon, strength is considerably larger than in ^{144}Nd for this level; however, the 4_1^+ ground-state decays of 12 W.u. for ^{144}Nd [5] and 14. W.u. for ^{142}Ce [32] are nearly the same.

Cottle *et al.* [5] have extensively investigated the vibrational versus $2qp$ character of the 4_1^+ state in ^{144}Nd. From the analyses of their (p,p') scattering data they conclude that the 4_1^+ state contains significant quantities of both $2qp$ and two quadrupole-phonon components which supports Gupta's assertion, i.e., that the collective nature of the 4_1^+ level is not developed away from its more particlelike nature in the $N=82$ nuclei. The $2qp$ nature of the 4_1^+ state, at least in the core $N=82$ nuclei, comes from coupling protons in the $d_{5/2}$ and $g_{7/2}$ orbits [5]. Pignanelli *et al.* [6] observe a significant $E4$ excitation to this level which suggests that 1-step processes are important in the excitation of this level, since

2-step excitations must be quite weak in (p,p') and (α,α') measurements.

As was discussed previously in Ref. [16], the enhanced collective nature of the 4_1^+ state in ^{142}Ce may result from the number of active protons participating in the interaction. Calculations for the $N=84$ isotones by Copnell *et al.* [13] indicate that there are more active protons in ^{142}Ce than in ^{144}Nd because of the subshell closure at $Z=64$.

3. Three-quadrupole phonon structures

The three-quadrupole phonon $(3Q)$ strength is expected to be spread in energy and probably fragmented among various levels because of the large anharmonicities obvious in the two-phonon structure. Signatures of these $3Q$ states are strong $E2$ decays into the two-phonon triplet and energies near three times the energy of the 2_1^+ state, i.e., at $\approx$2100 keV in ^{144}Nd. Below we list our best candidates for the $3Q$ quintuplet.

3Q 0^+ state. States with $J^\pi=0^+$ are observed at 2328.2, 2675.6, and 2743.2 keV. Only the 2743.2-keV state is observed to decay to any level other than the 2_1^+; specifically, it also decays into the 2_2^+. The rather large $E2$ transition rate for this decay of 14 W.u. makes this the best 0^+ candidate for the $3Q$ quintuplet.

3Q 2^+ state. Several 2^+ levels below 2.9 MeV are observed to decay into the 2_2^+ state, including those at 2527.8, 2592.5, 2693.0, (2829.3), and 2839.5 keV. The lowest of these which is also observed to decay into the 4_1^+ state is the level at 2693.0 keV. Upper limits on these decays are 2.4 W.u. for the decay into the 2_2^+ state and 11 W.u. for the decay into the 4_1^+ level.

3Q 3^+ state. The lowest 3^+ level is at 2178.8 keV and is observed to decay into the 4_1^+ state. No multipole-mixing ratio could be determined for this decay so the transition rate is unknown. Other higher-lying 3^+ levels are observed to decay into either the 2_2^+ or 4_1^+ levels, but just as for the 4_1^+ state, transition rates are not known.

3Q 4^+ state. Several 4^+ levels are observed which decay into either or both of the 2_2^+ and 4_1^+ levels. The lowest energy 4^+ state decaying into both these two-phonon states with significant $E2$ transition rates is the level at 2295.5 keV; however, only upper limits are given for these decays.

3Q 6^+ state. Spin-6 states occur at 1791.5, 2218.5, and 2808.8 keV. The 1791.5 keV level is the most like $3Q$ candidate because of its energy. It is observed to decay into the 4_1^+ by the emission of a 476.9 keV γ ray. Unfortunately, the energy of this γ ray is so low that it prohibits a lifetime measurement using DSAM.

VI. SUMMARY

The excited levels of ^{144}Nd below 3.3 MeV have been studied using the $(n,n'\gamma)$ reaction. Excitation functions, angular distributions, and Doppler shifts were measured for γ rays from these levels. Level lifetimes and spins, multipole-mixing and branching ratios, and electromagnetic transition rates were deduced. Nine new levels and over 30 new transitions assigned to existing levels were found below 3.3 MeV excitation.

The fragmentation of the lowest MS modes of excitation was investigated in ^{144}Nd. Experimental $B(M1)$ and $B(E2)$ transition rates and $E2/M1$ multipole-mixing ratios were examined from MS candidates into the lowest symmetric state, i.e., the 2_1^+ state. Both the 2_3^+ and 2_4^+ levels exhibit decay characteristics predicted for 2^+ MS excitations. There is weaker experimental evidence that the MS mode is spread into the 2_5^+ and into the 2_2^+ levels. Comparisons of these results for ^{144}Nd with analogous measurements reported earlier for 2^+ states in ^{142}Ce show that in both these nuclei there is strong experimental evidence supporting the fragmentation of the 2^+ MS mode of excitation into primarily the 2_3^+ and 2_4^+ levels, even though these levels are separated by over 300 keV. The MS mode was also investigated in 1^+ and 3^+ levels in ^{144}Nd. The 1^+ level at 2655.6 keV does exhibit a relatively fast $M1$ transition to the ground state of ^{144}Nd; however, more experimental information is needed to address MS strength in this state and fragmentation of the 1^+ MS mode. The experimental situation for 3^+ levels in ^{144}Nd is similar to that of the 1^+ levels. The 3_1^+ at 2178.8 keV exhibits decays similar to those predicted for MS states but information needed to assess MS fragmentation is not available.

Wave functions calculated using the IBM-2 support the fragmentation of MS strength in the 2_3^+ and 2_4^+ levels, as well as in the 2_5^+ state, although the model $B(M1)$ values for decays of the 2_4^+ and 2_5^+ states into the lowest 2^+ symmetric state are very small. The model also predicts that even though the lowest 1^+ and 3^+ state wave functions have dominant MS components, the $M1$ rates are not significantly larger than single-particle estimates. This model does an excellent job reproducing the measured transition rates from the 2_1^+ and 2_2^+ states, but underpredicts the ground-state decays of the 2_3^+ and 2_4^+ states. Some features, such as these ground-state decays of higher lying 2^+ states, lie outside the limits of the IBM-2 model and appear to require a more particlelike interpretation. For spin-3 states no clear identification of MS candidates can be made from the experimental information, but IBM-2 calculations show clearly that the MS strength is expected to be split between the first and second 3^+ states.

Existing CVM and QPM calculations were compared to our experimental data for transitions from low-lying 2^+ states in ^{144}Nd. Both of these models predict that MS strength is split between the 2_2^+ and 2_3^+ levels. This seems to differ from the experimental situation when traditional MS characteristics are used to assess MS strength in excited levels, e.g., unusually large $M1$ decays to the lowest symmetric state and small multipole-mixing ratios. There is, however, better overall agreement between calculated and experimental transition rates from these two models than from the IBM-2 which puts most of the 2^+ MS strength in the 2_3^+ and 2_4^+ levels. Calculations from these models need to be extended to higher-lying 2^+ levels and include 1^+ and 3^+ states in order to evaluate better the role of MS excitations in this nucleus and the agreement of the model predictions with experimental information. Comparisons between our expanded ^{144}Nd data set and existing PCM calculations show rather good agreement for some transitions, but appear to indicate that the model does not contain enough collective

strength. This is most obvious in members of the two-phonon triplet.

Lastly, we have investigated multiphonon excitations in ^{144}Nd. Evidence is given to support the 2779.0-keV level as the 3^- member of the QOC quintuplet and to propose that this mode of excitation is shared with the 2606.0-keV level. These assignments are based on new decay information for transitions into the 2_1^+ and 3_1^- levels. Transition rates measured for other previously proposed members of this quintuplet are found to be in excellent agreement with existing information. Levels exhibiting predicted decay characteristics for two- and three-quadrupole phonon states are also discussed.

ACKNOWLEDGMENTS

Insightful discussions with S.W. Yates, M.T. McEllistrem, and Marcel Villani are gratefully acknowledged. This work was supported by the National Science Foundation through Grants No. PHY-9303345 and No. PHY-9302914.

[1] J. K. Tuli, Nucl. Data Sheets **56**, 607 (1989).
[2] A. Ahmad, G. Bomar, H. Crowell, J. H. Hamilton, H. Kawakami, C. F. Maguire, W. G. Nettles, R. B. Piercey, A. V. Ramayya, and R. Soundranayagam, Phys. Rev. C **37**, 1836 (1988).
[3] R. H. Spear, W. J. Vermeer, S. M. Burnett, G. J. Gyapong, and C. S. Lim, Aust. J. Phys. **42**, 345 (1989).
[4] R. A. Meyer, O. Scholten, S. Brant, and V. Paar, Phys. Rev. C **41**, 2386 (1990).
[5] P. D. Cottle, S. M. Aziz, K. W. Kemper, M. L. Owens, E. L. Reber, J. D. Brown, E. R. Jacobsen, and Y. Y. Sharon, Phys. Rev. C **43**, 59 (1991).
[6] M. Pignanelli, N. Blasi, J. A. Bordewijk, R. De Leo, M. N. Harakeh, M. A. Hofstee, S. Micheletti, R. Perrino, V. Yu. Ponomarev, V. G. Soloviev, A. V. Sushkov, and S. Y. van der Werf, Nucl. Phys. **A559**, 1 (1993).
[7] R. Perrino, N. Blasi, R. De Leo, M. N. Harakeh, C. W. de Jager, S. Micheletti, J. Mieremet, M. Pignanelli, V. Yu. Ponomarev, R. K. L. Sandor, and H. de Vries, Nucl. Phys. **A561**, 343 (1993).
[8] S. J. Robinson, J. Jolie, H. G. Börner, P. Schillebeeckx, S. Ulbig, and K. P. Lieb, Phys. Rev. Lett. **73**, 412 (1994).
[9] T. Eckert, O. Beck, J. Besserer, P. Von Brentano, R. Fischer, R.-D. Herzberg, U. Kneissl, J. Margraf, H. Maser, A. Nord, N. Pietralla, H. H. Pitz, S. W. Yates, and A. Zilges, Phys. Rev. C **56**, 1256 (1997).
[10] W. D. Hamilton, A. Irbäck, and J. P. Elliott, Phys. Rev. Lett. **53**, 2469 (1984).
[11] Roland Nojarov and Amand Faessler, J. Phys. G **13**, 337 (1987).
[12] P. O. Lipas, P. von Brentano, and A. Gelberg, Rep. Prog. Phys. **53**, 1355 (1990).
[13] J. Copnell, S. J. Robinson, J. Jolie, and K. Heyde, Phys. Rev. C **46**, 1301 (1992).
[14] Thai Khac Dinh, M. Grinberg, and C. Stoyanov, J. Phys. G **18**, 329 (1992).
[15] W. J. Vermeer, C. S. Lim, and R. H. Spear, Phys. Rev. C **38**, 2982 (1988).
[16] J. R. Vanhoy, J. M. Anthony, B. M. Haas, B. H. Benedict, B. T. Meehan, Sally F. Hicks, C. M. Davoren, and C. L. Lundstedt, Phys. Rev. C **52**, 2387 (1995).
[17] F. Iachello, Phys. Rev. Lett. **53**, 1427 (1984).
[18] B. Fazekas, T. Belgya, G. Molnár, Á. Veres, R. A. Gatenby, S. W. Yates, and T. Otsuka, Nucl. Phys. **A548**, 249 (1992) and references therein.
[19] E. Sheldon and D. M. van Patter, Rev. Mod. Phys. **38**, 143 (1966).
[20] H. S. Camarda, T. W. Phillips, R. M. White, Phys. Rev. C **29**, 2106 (1984).
[21] K. B. Winterbon, Nucl. Phys. **A246**, 293 (1975).
[22] T. Belgya, B. Fazekas, G. Molnár, R. A. Gatenby, E. L. Johnson, E. M. Baum, D. Wang, D. P. DiPrete, and S. W. Yates, in *Proceedings of the 8th International Symposium on Capture Gamma-Ray Spectroscopy and Related Topics*, Fribourg, Switzerland, 1993, edited by J. Kern (World Scientific, Singapore, 1994), p. 878.
[23] T. Belgya, G. Molnár, and S. W. Yates, Nucl. Phys. **A607**, 43 (1996).
[24] T. Eckert, O. Beck, J. Besserer, P. Von Brentano, R. Fischer, R.-D. Herzberg, U. Kneissl, J. Margraf, H. Maser, A. Nord, N. Pietralla, H. H. Pitz, S. W. Yates, and A. Zilges, Phys. Rev. C **57**, 1007 (1998).
[25] T. J. Al-Janabi, J. D. Jafar, K. M. Mahmood, and H. M. Youhana, Nucl. Phys. **A402**, 247 (1983).
[26] D. M. Snelling and W. D. Hamilton, J. Phys. G **9**, 763 (1983).
[27] L. K. Peker, Nucl. Data Sheets **43**, 579 (1984).
[28] S. J. Robinson, J. Jolie, and J. Copnell, in *Capture Gamma-ray Spectroscopy*, Proceedings of the 7th International Symposium on Capture Gamma-Ray Spectroscopy and Related Topics, Asilomar, California, 1990, edited by Richard W. Hoff, AIP Conf. Proc. **238** (AIP, New York, 1991), 210.
[29] T. Otsuka and N. Yoshida, Japanese Atomic Energy Research Institute Report 85-094 (1985).
[30] S. J. Robinson, J. Copnell, J. Jolie, U. Stöhlker, and V. Rabbel, in *Proceedings of the 6th International Symposium on Capture Gamma-Ray Spectroscopy*, Leuven, Belgium, 1987, edited by K. Abrahams and P. Van Assche, IOP Conf. Series No. 88 (IOP, London, 1987), p. 506.
[31] M. Sambataro, O. Scholten, A. E. L. Dieperink, and G. Piccitto, Nucl. Phys. **A423**, 333 (1984).
[32] W. Kim, J. R. Calarco, J. P. Connelly, J. H. Heisenberg, F. W. Hersman, T. E. Milliman, J. E. Wise, B. L. Miller, C. N. Papanicolas, V. Yu. Ponomarev, E. E. Saperstein, and A. P. Platonov, Phys. Rev. C **44**, 2400 (1991).
[33] M. Behar, Z. W. Grabowski, and S. Raman, Nucl. Phys. **A219**, 516 (1974).
[34] P. Vogel and L. Kocbach, Nucl. Phys. **A176**, 33 (1971).
[35] F. R. Metzger, Phys. Rev. C **14**, 543 (1976).
[36] R. A. Gatenby, J. R. Vanhoy, E. M. Baum, E. L. Johnson, S. W. Yates, T. Belgya, B. Fazekas, Á. Veres, and G. Molnár, Phys. Rev. C **41**, R414 (1990).

[37] P. D. Cottle, S. M. Aziz, J. D. Fox, K. W. Kemper, and S. L. Tabor, Phys. Rev. C **40**, 2028 (1989).
[38] F. R. Metzger, Phys. Rev. **187**, 1700 (1969).
[39] N. Tsoneva, M. Grinberg, and Ch. Stoyanov, in *Proceedings of the 9th International Symposium on Capture Gamma-Ray Spectroscopy and Related Topics*, Budapest, Hungary, 1996, edited by G.L. Molnár, T. Belgya, and Zs. Révay (Springer, Budapest, 1997), p. 76.
[40] M. Pignanelli, N. Blasi, S. Micheletti, R. De Leo, M. A. Hofstee, J. M. Schippers, S. Y. van der Werf, and M. N. Harakeh, Nucl. Phys. **A519**, 567 (1990).
[41] P. D. Cottle, K. W. Kemper, M. A. Kennedy, L. f. Fifield, and T. R. Ophel, Phys. Rev. C **47**, 1048 (1993).
[42] J. K. Jewell, O. J. Tekyi-Mensah, P. D. Cottle, J. Döring, P. V. Green, J. W. Holcomb, G. D. Johns, T. D. Johnson, K. W. Kemper, P. L. Kerr, S. L. Tabor, P. C. Womble, and V. A. Wood, Phys. Rev. C **52**, 1295 (1995).
[43] J. B. Gupta, Nucl. Phys. **A484**, 189 (1988).